



1 **Direct measurement of N₂O₅ heterogeneous uptake**
2 **coefficients on atmospheric aerosols in southwestern**
3 **China and evaluation of current parameterizations**

4 Jiayin Li ^{a,†}, Tianyu Zhai ^{a,b,†}, Xiaorui Chen ^{c,*}, Haichao Wang ^c, Shuyang Xie ^a, Shiyi
5 Chen ^a, Chunmeng Li ^{a,d}, Huabin, Dong ^a, Keding Lu ^{a,*}

6

7 ^a State Key Joint Laboratory of Environmental Simulation and Pollution Control,
8 College of Environmental Science and Engineering, Peking University, Beijing 100871,
9 China

10 ^b State Environmental Protection Key Laboratory of Vehicle Emission Control and
11 Simulation, Chinese Research Academy of Environmental Sciences, Beijing, 100012,
12 China

13 ^c School of Atmospheric Sciences, Sun Yat-sen University, and Southern Marine
14 Science and Engineering Guangdong Laboratory (Zhuhai), Zhuhai, 519082, China

15 ^d The National Institute of Metrology, Center for Environmental Metrology, Beijing
16 100029, China

17 [†]Jiayin Li and Tianyu Zhai contributed equally in this work.

18

19 **Corresponding author:** Xiaorui Chen (chenxr95@mail.sysu.edu.cn) and Keding Lu
20 (k.lu@pku.edu.cn)

21

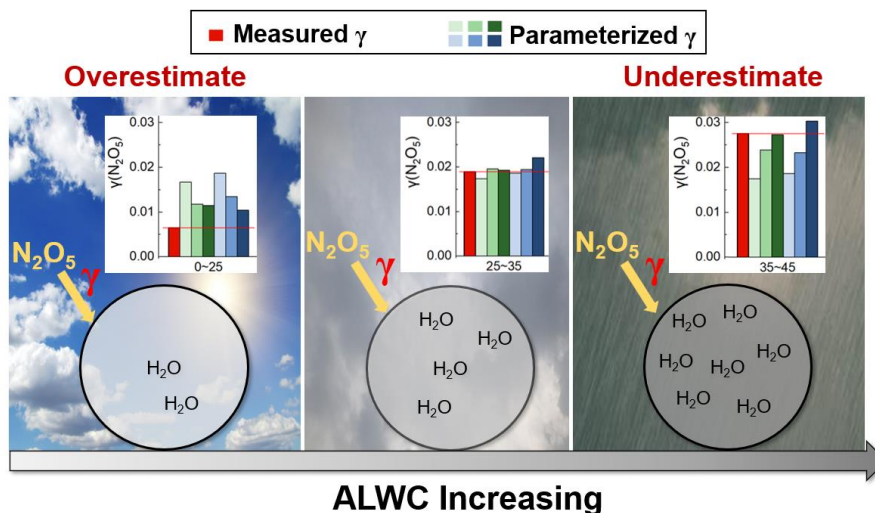
22 **Abstract:** The heterogeneous hydrolysis of dinitrogen pentoxide (N₂O₅) is a critical
23 process in assessing NO_x fate and secondary pollutants (e.g. particulate nitrate)
24 formation. However, accurate quantification of the N₂O₅ uptake coefficient ($\gamma(\text{N}_2\text{O}_5)$)
25 in the ambient conditions is a challenging problem which can causes unpredictable
26 uncertainties in the predictions of the air quality models. Here, the $\gamma(\text{N}_2\text{O}_5)$ values were
27 directly measured using an improved aerosol flow tube system in a city located on the
28 plateau in southwestern China to investigate its influencing factors and the performance
29 of current $\gamma(\text{N}_2\text{O}_5)$ parameterization under this typical environmental condition. The
30 nocturnal mean $\gamma(\text{N}_2\text{O}_5)$ value ranged from 0.0018 to 0.12 with an average of
31 0.023 ± 0.021 . The aerosol water significantly promoted N₂O₅ uptake, while particulate
32 organic and nitrate generally showed suppression effect. We found that median $\gamma(\text{N}_2\text{O}_5)$



33 predicted by some parameterizations agreed well with observation, whereas the
 34 parameterizations failed to reproduce the range of observed values and showed poor
 35 correlations ($R^2=0.00\sim0.09$). Elevated differences between prediction and observation
 36 specifically occurred at high aerosol liquid water content (ALWC) with an
 37 underestimation by $-37\%\sim-1\%$ and low ALWC with an overestimation by $34\sim189\%$,
 38 respectively. Such differences between the measured and parameterized $\gamma(N_2O_5)$ would
 39 lead to biased estimation ($-77\%\sim74\%$) on particulate nitrate production potential. Our
 40 findings suggest the need for more direct field quantifications of $\gamma(N_2O_5)$ and the
 41 laboratory measurements under extreme ALWC conditions to re-evaluate the response
 42 coefficients between $\gamma(N_2O_5)$ and aerosol chemical compositions.

43 **Keywords:** N_2O_5 uptake coefficient, $\gamma(N_2O_5)$ parameterizations, particulate nitrate
 44 formation, nighttime chemistry

45



46

47

48

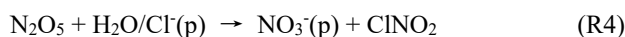
49

50 1. Introduction

51 Nitrate radical (NO_3) and dinitrogen pentoxide (N_2O_5) are dominant in nocturnal
 52 atmospheric chemistry as reactive nitrogen species that can strongly influence the
 53 concentration and distribution of ozone (O_3) and nitrogen oxides ($NO_x=NO+NO_2$), and



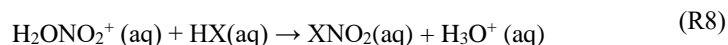
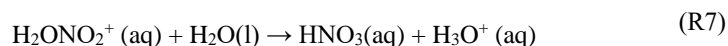
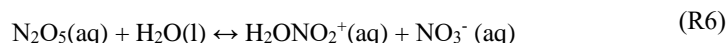
54 the air quality (Brown et al., 2006; Wang et al., 2023; Decker et al., 2019; Dentener and
55 Crutzen, 1993). NO_3 is produced by the reaction of NO_2 and O_3 (R1), and there is a
56 thermodynamic equilibrium between NO_3 and N_2O_5 (R2), which is the source of N_2O_5
57 (Brown and Stutz, 2012). There are two main pathways for NO_3 removal: the direct one
58 is reactions of NO_3 and VOCs (R3), especially alkenes, and the indirect way is the
59 heterogenous hydrolysis of N_2O_5 (Asaf et al., 2009; Ng et al., 2017). N_2O_5 can react
60 with H_2O and chloride (Cl^-) in the particle phase and form soluble nitrate and nitryl
61 chloride (ClNO_2) (R4) (Osthoff et al., 2008; Chang et al., 2011). The uptake of N_2O_5
62 is the main pathway for the formation of particulate nitrate at night, which contributes to
63 $\text{PM}_{2.5}$ (<2.5 μm in diameter) pollution. Meanwhile, chlorine radical is produced by
64 ClNO_2 photodecomposition in daytime and further regulate the O_3 pollution production
65 by promoting the oxidation of VOCs (Finlaysonpitts et al., 1989; Riedel et al., 2014).
66 Thus, it is important to quantify the rate of the N_2O_5 heterogeneous hydrolysis reaction
67 in ambient conditions.



68 $\gamma(\text{N}_2\text{O}_5)$ is defined as the net probability of N_2O_5 irreversibly taken up onto an
69 aerosol surface upon collision (McDuffie et al., 2018). According to previous study, the
70 process of N_2O_5 heterogeneous hydrolysis reaction on aerosols was treated as a resistor
71 model including three steps: gas diffusion (R5), surface accommodation, and aqueous
72 reaction (R6~R8) (Abbatt et al., 2012; Fang et al., 2024). This process can be influenced
73 by aerosol chemical compositions (e.g. aerosol liquid water content (ALWC), nitrate
74 (NO_3^-) concentration, Cl^- concentration, and organics), morphology and ambient
75 meteorological factors (Bertram and Thornton, 2009; Mozurkewich and Calvert,
76 1988; Roberts et al., 2009; Thornton et al., 2003). High concentration of ALWC and Cl^-
77 can promote the uptake reaction (R6~R8), and NO_3^- suppress the reaction (R6).
78 Organics also can suppress the reaction by forming a coating on the surface of the
79 particles and regulating the ALWC and the passage rate of N_2O_5 molecules (Folkers et
80 al., 2003; Gaston et al., 2014; Anttila et al., 2006). However, the above results are mainly
81 based on laboratory studies. In ambient conditions, the correlations between $\gamma(\text{N}_2\text{O}_5)$
82 and aerosol chemical compositions were generally weak mainly due to the coupling



83 effects of particle morphology, size, mixing state, and meteorological parameters (e.g.
84 temperature and relative humidity) (Phillips et al., 2016; Wang et al., 2020b; Riedel et
85 al., 2012).



86 In order to accurately quantify the contribution of N_2O_5 heterogeneous hydrolysis
87 to nitrate formation and NO_x regulation, a variety of parameterizations of $\gamma(\text{N}_2\text{O}_5)$ have
88 been established based on laboratory and field studies (Evans and Jacob, 2005; Davis et
89 al., 2008; Yu et al., 2020; Bertram and Thornton, 2009). The parameters in
90 parameterizations mainly include the meteorological parameters, concentrations of
91 aerosol chemical compositions, and particle physicochemical parameters. However, the
92 comparisons of parameterized and measured $\gamma(\text{N}_2\text{O}_5)$ in field measurements revealed
93 significant discrepancies between them (Brown et al., 2009; Ryder et al.,
94 2014; McDuffie et al., 2018), which mainly lie in the large variations in response of
95 $\gamma(\text{N}_2\text{O}_5)$ to particle compositions on ambient particles. Moreover, the overestimation or
96 underestimation of the parameterized $\gamma(\text{N}_2\text{O}_5)$ can lead to unpredictable biases in the
97 simulations of the chemical transport models (Murray et al., 2021; Chen et al.,
98 2018; Ryder et al., 2014).

99 Until now, only a few studies have quantified $\gamma(\text{N}_2\text{O}_5)$ values in ambient conditions
100 ($<10^{-4}$ to 0.1) mostly by indirect quantification methods (Brown et al., 2016; Wang et
101 al., 2018; Chen et al., 2020b; Morgan et al., 2015; Tham et al., 2018) while some by direct
102 measurements (Yu et al., 2020; Riedel et al., 2012; Bertram et al., 2009a). The N_2O_5
103 heterogeneous uptake process has been reported to be active in China. The $\gamma(\text{N}_2\text{O}_5)$
104 values in North China Plain, Yangtze River Delta and Pearl River Delta in China (10^{-2}
105 $\sim 10^{-1}$) were generally about 1 to 2 orders of magnitude larger than that in European
106 and North America ($10^{-3} \sim 10^{-2}$) (Yan et al., 2023; Wang et al., 2017b; Wang et al.,
107 2017d; Wang et al., 2017c; Niu et al., 2022). To further investigate the N_2O_5
108 heterogeneous chemistry in China, the $\gamma(\text{N}_2\text{O}_5)$ values were directly measured in a
109 typical highland city, Kunming, in China using an improved aerosol flow tube system
110 from 15 April to 20 May 2021. The relationship between the $\gamma(\text{N}_2\text{O}_5)$ values and
111 impacting factors was determined. We then examine the performance of current $\gamma(\text{N}_2\text{O}_5)$



112 parameterizations by comparing to the observed values and analyze the causes of
113 discrepancies in extreme ALWC conditions. We further notice the significant biases of
114 particulate nitrate formation potential estimated by $\gamma(\text{N}_2\text{O}_5)$ parameterization.

115 2. Methods

116 2.1. Site description

117 The field campaign was conducted in Kunming, China from 15 April to 20 May
118 2021. The main sampling site was on the roof of the Yihe Building, Yijingyuan Hotel
119 ($24^\circ59'05''$ N, $102^\circ39'40''$ E), about 20 m above the ground. As shown in Figure 1, the
120 measurement site was located approximately 1890 m above sea level, 8 km away from
121 the city center, and 1 km from Dianchi Lake to the west. The site receives traffic
122 emissions from two roads within a radius of 500 m. The site was mainly surrounded by
123 residential area and there was no major industrial source around. Besides, the particle
124 composition was measured at Guandu Forest Park ($25^\circ00'43''$ N, $102^\circ45'55''$ E), which
125 was about 9 km away from Yijingyuan Hotel, 5.2 km from the city center and was also
126 mainly surrounded by residential living area. Sunrise was around 06:30 CNST and
127 sunset at 19:30 CNST.



128

129 **Figure 1. Google Maps images showing the locations of the experimental sites.**

130 (a) The location of the Yijingyuan Hotel and Guandu Forest Park. (b) The surrounding
131 environment of Yijingyuan Hotel.

132 2.2. Instrument setup

133 Multiple gas phase and particulate parameters were measured during the campaign,
134 including N_2O_5 , NO, NO_2 , O_3 , VOCs, $\text{PM}_{2.5}$, particle number size distribution (PNSD),
135 particle composition, and meteorological parameters. The detailed information of the
136 instruments is listed in Table 1.



137 N_2O_5 concentration was measured by a cavity-enhanced absorption spectrometer
 138 (CEAS) developed by Wang et al. (Wang et al., 2017a), and has been used in several
 139 field campaigns. N_2O_5 in the sampling gas was thermally decomposed to NO_3 in a
 140 preheated perfluoroalkoxy alkane (PFA) tube (130 °C), and then detected in a resonator
 141 cavity maintained at 110 °C to avoid the reversible reaction of N_2O_5 and NO_3 . Excess
 142 NO was injected to the cavity every 5 min to obtain the reference spectrum by
 143 eliminating the influence of water vapor. The N_2O_5 loss in the sampling system and
 144 detection system were also calibrated and corrected during data processing. The
 145 detection of limit (LOD) of CEAS was 2.7 pptv (1σ), and the uncertainty was 19%.

146 NO , NO_2 and O_3 were monitored by commercial instruments (Thermo-Fisher 42i
 147 and 49i). A total of 117 kinds of volatile organic compounds (VOCs) were measured by
 148 an automated gas chromatograph equipped with a mass spectrometer and flame
 149 ionization detector (GC-MS/FID). The particle composition was measured by a time-
 150 of-flight aerosol chemical speciation monitor (ToF-ACSM), including sulfate, nitrate,
 151 ammonium, chloride and organics. The ALWC was calculated by ISORROPA-II model
 152 and did not consider the hygroscopicity of organic compounds (Fountoukis and Nenes,
 153 2007). PNSD were measured by a scanning mobility particle sizer (SMPS, TSI Model
 154 3938) including an Electrostatic Classifier (Model 3082) and a condensation particle
 155 counter (CPC, Model 3776). Meteorological parameters, included relative humidity
 156 (RH), temperature (T), pressure, wind speed and wind direction, were available during
 157 the campaign.

158 Table 1. The detailed information of instruments during the campaign.

Parameters	Detection of limit	Method	Accuracy
N_2O_5	2.7 pptv (1σ , 1min)	CEAS	\pm 19%
NO	50 pptv (2min)	Chemiluminescence	\pm 10%
NO_2	50 pptv (2min)	Chemiluminescence ^a	\pm 10%
O_3	0.5 ppbv (2σ , 1min)	UV photometry	\pm 5%
VOCs	2–190 ppt (1 h)	GC-MS/FID	\pm 5%
PNSD	14–730 nm (5 min)	SMPS	\pm 10%
Particle composition	m/z 10 – 219 (10 min)	ToF-ACSM	-
$\gamma(\text{N}_2\text{O}_5)$	0.0016 (40 min)	Aerosol flow tube system	\pm 16–43 %

159 ^a Photolytic conversion to NO through blue light before detection.



160 **2.3. The measurement and calculation of $\gamma(\text{N}_2\text{O}_5)$**

161 The $\gamma(\text{N}_2\text{O}_5)$ was directly measured by an aerosol flow tube system (AFTS)
162 coupled with a detailed box model developed by Chen et al. (Chen et al., 2022). The
163 detection limit and accuracy of the AFTS are listed in Table 1. Briefly, the AFTS mainly
164 consists of a N_2O_5 generator, an aerosol flow tube, and detection instruments for N_2O_5 ,
165 NO_x , O_3 and S_a . N_2O_5 generated by O_3 and NO_2 (excess) was added to the sampling gas
166 in the front of the aerosol flow tube. The aerosol flow tube consist of two cones at both
167 ends with a vertex angle of 15° and a straight cylinder in the middle with an inner
168 diameter of 140 mm and a length of 343 mm. The total flow rate in the tube was 2.08
169 L min^{-1} , and the residence time was 259 s. The detection instruments used in this study
170 were Thermo 42i-TL to detect NO and NO_2 concentration, Teledyne T265 to detect O_3
171 concentration, CEAS-PKU to detect N_2O_5 concentration and SMPS (TSI Model 3938)
172 to detect aerosol surface concentrations (S_a). Meanwhile, a RH&T sensor (Rotronic,
173 Model HC2A-S) was used to detect relative humidity and temperature in the flow tube.
174 In a duty cycle, the N_2O_5 concentrations with or without aerosols were acquired at both
175 the inlet and exit of the flow tube, NO , NO_2 and O_3 concentrations were always acquired
176 at the inlet, S_a concentration always acquired at the exit. The loss rate coefficients of
177 N_2O_5 were calculated by a time-dependent box model coupled with NO_3 - N_2O_5
178 chemistry under the constraint of the measurement of N_2O_5 concentrations and other
179 auxiliary parameters to overcome the influence of homogeneous reactions (e.g., NO_2 ,
180 O_3 and NO) and variations of air mass on $\gamma(\text{N}_2\text{O}_5)$ retrieval. The N_2O_5 loss rate in the
181 absence of aerosols was expected as wall loss rate coefficients ($k_{het}^{wo/aerosols}$) of N_2O_5 ,
182 and the loss rate in the presence of aerosols was expected as the loss rate both on wall
183 and aerosols ($k_{het}^{w/aerosols}$) of N_2O_5 . Therefore, $\gamma(\text{N}_2\text{O}_5)$ could be calculated by Eq (1).
184 Among them, the loss of S_a concentration in aerosol flow tube was corrected by the
185 penetration efficiency derived in our previous study (Chen et al., 2022) and the dry-
186 state S_a were corrected to ambient (wet) S_a by a hygroscopic growth factor (Liu et al.,
187 2013). A stringent data QA/QC procedure is applied prior to model calculation based
188 on above measured variables to retrieve robust $\gamma(\text{N}_2\text{O}_5)$ values. Other detailed
189 information about this system can be found in Chen et al. 2022.



$$\gamma(N_2O_5) = \frac{4 \times (k_{het}^{w/aerosols} - k_{het}^{wo/aerosols})}{c \times S_a} \quad (1)$$

190 2.4 The calculation of NO₃ and N₂O₅ reactivity

191 NO₃ production rate (P(NO₃)) was calculated by measured NO₂ concentration and
 192 O₃ concentration via Eq.(2), $k_{NO_2+O_3}$ represents the reaction rate of constant of NO₂
 193 and O₃ (Atkinson et al., 2004). NO₃ concentration can be calculated by measured N₂O₅
 194 concentration with the temperature-dependent equilibrium relationship (Eq.3). The
 195 steady-state lifetime of N₂O₅ ($\tau(N_2O_5)$) and NO₃ ($\tau(NO_3)$) was calculated by
 196 concentrations and P(NO₃) as shown in Eq.(4) and Eq.(5) (Brown and Stutz, 2012). The
 197 NO₃ reactivity with VOCs ($k(NO_3)$) can be calculated by Eq.(6), among them k_i
 198 represents the bimolecular rate coefficients.

$$P(NO_3) = k_{NO_2+O_3}[NO_2][O_3] \quad (2)$$

$$[NO_3] = [N_2O_5]/k_{eq}[NO_2], \quad (3)$$

$$k_{eq} = 5.5 \times 10^{-27} \times e^{10724/T}$$

$$\tau(N_2O_5) = [N_2O_5]/P(NO_3) \quad (4)$$

$$\tau(NO_3) = [NO_3]/P(NO_3) \quad (5)$$

$$k(NO_3) = \sum k_i [VOC_i] \quad (6)$$

199 2.5 The calculation of nitrate production rate

200 The N₂O₅ uptake for nighttime particulate nitrate production is regarded as a
 201 pseudo first order reaction, the rate constant ($k_{N_2O_5}$) of which can be calculated from
 202 Eq 7 with measured or parameterized $\gamma(N_2O_5)$, where C is the mean molecular speed of
 203 N₂O₅. The yield ratio of ClNO₂ (ϕ) was set as a constant of 0.5 in all calculations, which
 204 is consistent with the previously observed yield range 0.3~0.73 in North China (Wang
 205 et al., 2017d; Wang et al., 2018). The nitrate production rate can be calculated by Eq 8,
 206 where $[N_2O_5]$ is the concentration of N₂O₅.

$$k_{N_2O_5} = 0.25 \times S_a \times \gamma(N_2O_5) \times C \quad (7)$$

$$P(NO_3^-) = k_{N_2O_5} \times [N_2O_5] \times (2-\phi) \quad (8)$$



207 **3. Results and discussion**

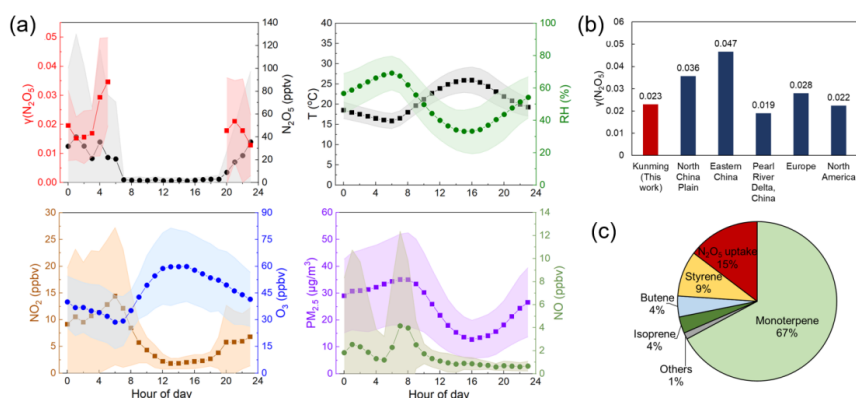
208 **3.1. $\gamma(\text{N}_2\text{O}_5)$ measurement overview and comparison**

209 The mean diurnal of measured N_2O_5 concentration, $\gamma(\text{N}_2\text{O}_5)$ values, RH, T,
210 concentrations of NO_2 , O_3 , NO , $\text{PM}_{2.5}$ from 15 April to 20 May 2021 are shown in
211 Figure 2a, and the time series are shown in Figure S1. Higher $\text{PM}_{2.5}$ concentration was
212 observed at night (average of $27.8 \pm 14.3 \text{ ug/m}^3$, peak of 81.0 ug/m^3) than that in the
213 day (Figure 2a & Figure S1). The NO_2 (average of $6.5 \pm 8.4 \text{ ppbv}$) and O_3 (average of
214 $45.5 \pm 19.7 \text{ ppbv}$) concentration in Kunming are lower than other regions in China
215 (Wang et al., 2017d; Wang et al., 2020a; Niu et al., 2022; Li et al., 2020), indicating a
216 lower atmospheric oxidation capacity. The mean nocturnal NO_3 production rate (PNO_3)
217 was $0.6 \pm 0.8 \text{ ppbv/h}$, which is also lower than previous reports in China (Tham et al.,
218 2016; Zhai et al., 2023; Wang et al., 2022). During this observation campaign, significant
219 N_2O_5 concentration (at a maximum of 395.1 pptv) was only observed within April 16-
220 27 mainly with low humidity and high precursor concentrations, while the
221 concentrations fluctuated around the detection limit during other periods. The nocturnal
222 mean concentration of N_2O_5 was $33.4 \pm 75.2 \text{ pptv}$, which is lower than reported
223 concentrations in other regions of China (Wang et al., 2018; Brown et al., 2016; Zhai
224 et al., 2023). During the field measurement, high temperature ($\sim 20^\circ\text{C}$) favors the
225 equilibrium shifting from N_2O_5 towards NO_3 and site mainly received the emissions
226 from vegetations in the surrounding parks. In that case, the major removal of NO_3 - N_2O_5
227 at night was the reaction of NO_3 with VOCs represented by monoterpene (67%) and
228 isoprene (4%), followed by N_2O_5 uptake (15%) shown in Figure 2c. Rapid depletion of
229 daytime emitted isoprene by NO_3 led to low contribution of isoprene to NO_3 reactivity
230 after sunset (Figure S2). The steady-state lifetime of N_2O_5 ($\tau(\text{N}_2\text{O}_5)$) was $185 \pm 294 \text{ s}$
231 on average and its diel pattern was similar to N_2O_5 concentration. The $\tau(\text{N}_2\text{O}_5)$ in
232 Kunming were higher than most other cities in China (Wang et al., 2020a; Li et al.,
233 2020; Yan et al., 2019). Comparisons of NO_3 and N_2O_5 concentrations, $\text{P}(\text{NO}_3)$, and
234 other parameters with that recently reported in other regions across the world are
235 summarized in Table S1.

236 The nocturnal mean $\gamma(\text{N}_2\text{O}_5)$ value ranged from 0.0018 to 0.12 with an average of
237 0.023 ± 0.021 . The diurnal profiles showed that the $\gamma(\text{N}_2\text{O}_5)$ value decreased after sunset
238 and then sharply increased with relative humidity after midnight, peaking at 5:00 am
239 (Figure 2a). The mean $\gamma(\text{N}_2\text{O}_5)$ was lower than that in North China Plain and Eastern



240 China, and similar to that in Pearl River Delta China, Europe and North America
 241 (Figure.2b) (Yan et al., 2023; Wang et al., 2017b; Wang et al., 2017d; Wang et al.,
 242 2017c; Niu et al., 2022; Morgan et al., 2015; Phillips et al., 2016; Bertram et al.,
 243 2009a; McDuffie et al., 2018). The detailed comparisons of field derived $\gamma(\text{N}_2\text{O}_5)$ were
 244 summarized in Table S2.



245
 246 **Figure 2. The overview of $\gamma(\text{N}_2\text{O}_5)$, gas phase and particulate parameters,**
 247 **meteorological parameters and NO_3 loss pathways.** (a) Mean diurnal profiles of
 248 measured $\gamma(\text{N}_2\text{O}_5)$, N_2O_5 , T , RH , NO_2 , O_3 , $\text{PM}_{2.5}$ and NO . (b) Comparison of $\gamma(\text{N}_2\text{O}_5)$
 249 values in China, Europe, and North America calculated from previous work with
 250 measured value in this work. (c) The percentage of NO_3 loss pathway via VOCs and
 251 N_2O_5 uptake at night.

252 3.2. Functional dependence of measured $\gamma(\text{N}_2\text{O}_5)$ values

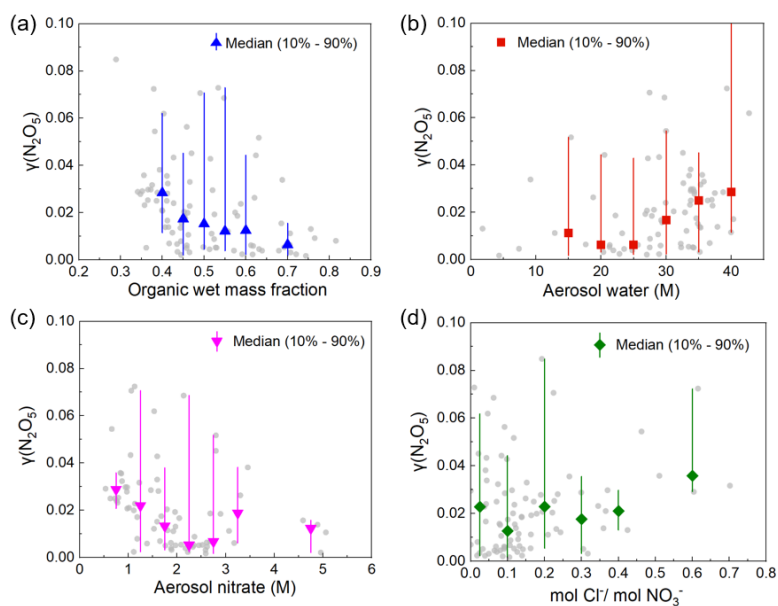
253 The dependence of measured $\gamma(\text{N}_2\text{O}_5)$ values on organics, ALWC, NO_3^- and Cl^-
 254 concentration in particle phase in this study are shown in Figure 3. The organic wet
 255 mass fraction showed a significant negative correlation ($R^2=0.83$) with measured
 256 $\gamma(\text{N}_2\text{O}_5)$ values (Figure 3a), indicating that organics in the aerosol significantly
 257 inhibited the uptake of N_2O_5 during the measuring period in Kunming. While a large
 258 number of studies have observed evident suppression of particulate organic on N_2O_5
 259 uptake on lab-generated aerosols (Escoreia et al., 2010; Cosman and Bertram,
 260 2008; Gaston et al., 2014), the negative correlation of particulate organic and $\gamma(\text{N}_2\text{O}_5)$
 261 was usually weak derived from field measurements (Brown et al., 2009; McDuffie et al.,
 262 2018; Chen et al., 2018; Wang et al., 2020b).

263 Aerosol liquid water also exhibited controlling role on heterogeneous uptake of
 264 N_2O_5 in this study as demonstrated by the evidently positive correlation ($R^2=0.74$) of



265 ALWC and $\gamma(\text{N}_2\text{O}_5)$ (Figure 3b). A weak correlation was observed with ALWC below
266 25 M and a significant correlation observed with ALWC higher than 25 M. The similar
267 trend has been reported by previous laboratory studies (Mozurkewich and Calvert,
268 1988; Bertram and Thornton, 2009; Folkers et al., 2003; Hallquist et al., 2003). When RH
269 is low, the aerosols mainly exist in solid state with low ALWC, limiting the uptake
270 reaction. Whereas the aerosols become deliquesced as the RH (also ALWC) increases,
271 which greatly promote the uptake reaction. Previous field studies also found good
272 correlations of $\gamma(\text{N}_2\text{O}_5)$ values with ALWC or RH in most regions in China, indicating
273 that ALWC may be one of the rate-limiting steps of heterogeneous reaction in China
274 (McDuffie et al., 2018; Yu et al., 2020; Tham et al., 2018; Wang et al., 2022).

275 Figure 3c showed the negative dependence of measured $\gamma(\text{N}_2\text{O}_5)$ values on aerosol
276 nitrate concentration, similar to the results of previous laboratory studies and most field
277 observations (Tham et al., 2018; Bertram et al., 2009b; Morgan et al., 2015; Yu et al.,
278 2020). The suppression effect of NO_3^- on the N_2O_5 heterogeneous uptake is mainly
279 caused by the competition of aerosol nitrate with chloride and H_2O for the H_2ONO_2^+
280 intermediate (Bertram and Thornton, 2009). The positive correlation ($R^2=0.48$)
281 between $\gamma(\text{N}_2\text{O}_5)$ and molar ratio of $\text{Cl}^-/\text{NO}_3^-$ values was weaker than that of ALWC
282 (Figure 3d), which indicates that Cl^- may promote the N_2O_5 uptake reaction instead of
283 playing a critical role during our observation. The particulate Cl^- concentration also
284 contributes to weaker enhancement of $\gamma(\text{N}_2\text{O}_5)$ compared to ALWC in other field
285 observations (Wang et al., 2020b; Yu et al., 2020; McDuffie et al., 2018).



286

287 **Figure 3. The functional dependence of measured $\gamma(\text{N}_2\text{O}_5)$ values on the**
 288 **influencing factors.** Variation of $\gamma(\text{N}_2\text{O}_5)$ with organic wet mass fraction (a), the
 289 aerosol water content (b), the aerosol nitrate content (c), and molar ratio of chloride to
 290 nitrate (d). The points represent the median in each bin, and the color lines represent
 291 the data range from 10th to 90th percentile in each bin.

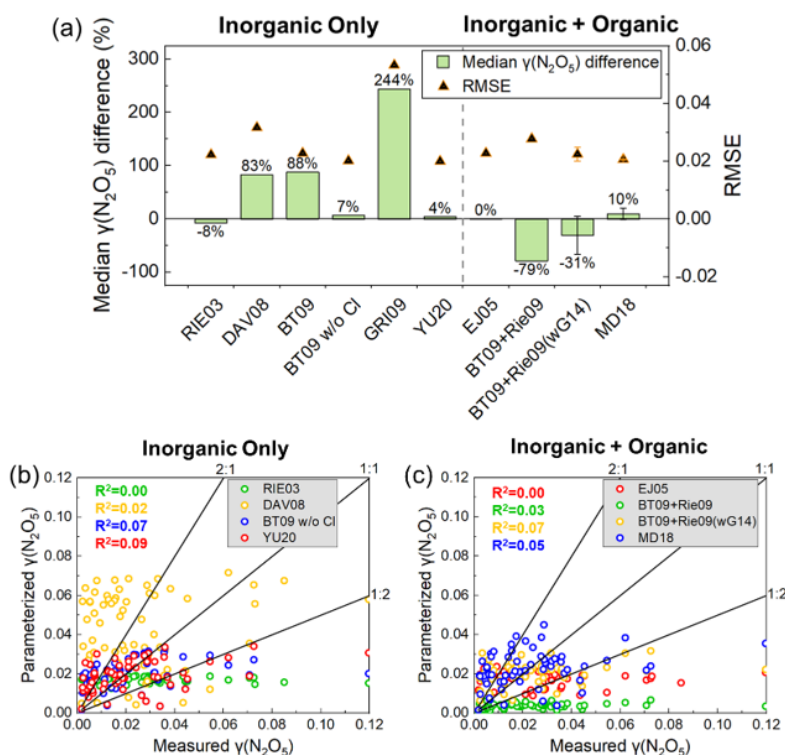
292 3.3. Comparison of parameterized $\gamma(\text{N}_2\text{O}_5)$ values

293 The $\gamma(\text{N}_2\text{O}_5)$ values were predicted using ten widely-used parameterizations and
 294 compared with the measured results. The details of the parameterizations were
 295 summarized in Table S3. Parameterizations were categorized into inorganic-only and
 296 inorganic kernel with organic coating or organic mass (inorganic+organic).

297 The $\gamma(\text{N}_2\text{O}_5)$ predicted by inorganic-only parameterizations were generally larger
 298 than measurements. Among these inorganic-only parameterizations, RIE03, BT09 w/o
 299 Cl and Yu20 exhibited relatively low deviation in predicted median values from
 300 measurements (Figure 4a). However, the correlation of predictions and measurements
 301 were bad for these three parameterizations ($R^2=0\sim 0.09$, Figure 4b). The empirical
 302 parameterization Yu20 derived from several field campaigns in China showed the best
 303 performance with a median difference of 4%, the lowest RMSE (0.0200) and the
 304 highest correlation coefficient ($R^2=0.09$) in Kunming, indicating the effectiveness of
 305 the improvement by the localized field results. The overestimation of the DAV08, BT09



306 and GRI09 were also reported by previous studies (Bertram et al., 2009b; Brown et al.,
 307 2009; Chang et al., 2016; Griffiths et al., 2009; McDuffie et al., 2018). All
 308 parameterizations had difficulty in predicting the low and high values of measured
 309 $\gamma(\text{N}_2\text{O}_5)$. For the parameterizations with median deviation less than 10%, the
 310 parameterized $\gamma(\text{N}_2\text{O}_5)$ values mainly fell in the range of 0.0036~0.035, while the
 311 measured values varied from 0.0018 to 0.12, indicating that the relevant parameters in
 312 the parameterizations was still inappropriate and cannot reproduce the range of the
 313 measurements.



314
 315 **Figure 4. Comparison of parameterized and measured $\gamma(\text{N}_2\text{O}_5)$.** (a) Comparison of
 316 median difference and root-mean-square-error (RMSE) between measured $\gamma(\text{N}_2\text{O}_5)$ and
 317 parameterized $\gamma(\text{N}_2\text{O}_5)$ values. The error bar of BT09+Rie09wG14 and MD18 showed
 318 the range of the results of O/C setting between 0.5 and 0.8. The distribution of
 319 parameterized $\gamma(\text{N}_2\text{O}_5)$ values, including inorganic-only parameterizations (RIE03,
 320 DAV08, BT09 w/o Cl, YU20) (b), and inorganic+organic parameterizations (EJ05,
 321 BT09+Rie09, BT09+Rie09wG14, MD18) (O/C=0.8) (c). The black solid line
 322 represents the 1:1, 1:2 and 2:1 line, respectively. The R^2 displayed in different colors



323 correspond to the parameterization of the same color.

324 The inorganic+organic parameterizations tend to underestimate the measured
325 $\gamma(\text{N}_2\text{O}_5)$ due to the suppression effects of organics. Worse agreement and larger scatter
326 were found for the parameterized $\gamma(\text{N}_2\text{O}_5)$ ($R^2=0\sim 0.07$, Figure 4c) when organics part
327 was added into inorganic. BT09+Rie09(wG14) showed the best correlation with R^2 of
328 0.07 but relatively large median deviation (-66~5%). EJ05 and MD18 showed the
329 lowest deviations among the four parameterizations, while EJ05 showed the worst
330 correlation ($R^2=0.00$). Among them, the empirical parameterization MD18, derived
331 from field observations, exhibited the best performance with a deviation of -1~20% and
332 the lowest RMSE (0.0207), which also indicates that parameterization can be improved
333 by fitting to field observations, similar to the results of inorganic-only
334 parameterizations.

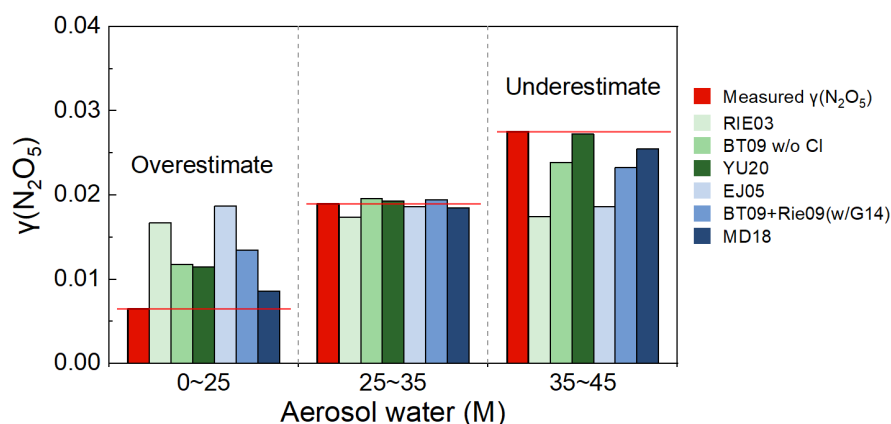
335 **3.4. The impact of ALWC on parameterized $\gamma(\text{N}_2\text{O}_5)$**

336 Although some parameterizations performed relatively well in reproducing the
337 median values of $\gamma(\text{N}_2\text{O}_5)$, none of the ten parameterizations were able to reproduce the
338 range of measured $\gamma(\text{N}_2\text{O}_5)$ values (aka. low correlation and RMSE). This phenomenon
339 was possibly caused by several aspects, including the inaccurate estimation on response
340 coefficients of critical aerosol compositions and relative rates of competitive reactions,
341 especially when influenced by organics components. ALWC is one of the factors
342 controlling N_2O_5 uptake during our observation and the coefficients related to ALWC
343 should play a critical role in reproducing the varying range of $\gamma(\text{N}_2\text{O}_5)$. To investigate
344 the accuracy of the ALWC-related response coefficients in $\gamma(\text{N}_2\text{O}_5)$ parameterizations,
345 we compared the parameterized and measured $\gamma(\text{N}_2\text{O}_5)$ values at three ALWC levels:
346 low concentration (0~25 M), medium concentration (25~35 M), and high concentration
347 (35~45 M).

348 Six parameterizations were selected for the comparison at different ALWC levels
349 due to their low deviations (below 10% of median values) over the entire observation
350 (Figure 5). At low ALWC, all six parameterizations showed overestimation with the
351 maximum difference for EJ05 (189%) and the minimum for MD18 (34%). At median
352 ALWC, the deviation of parameterized $\gamma(\text{N}_2\text{O}_5)$ reduced to -8~4%. At high ALWC, the
353 parameterizations tend to underestimate the measured $\gamma(\text{N}_2\text{O}_5)$ with the difference
354 ranging from -37% to -1%. The treatment of ALWC-related effects on the $\gamma(\text{N}_2\text{O}_5)$
355 following BT09 and Rie09 parameterizations framework were generally better than
356 those following RIE03 and EJ05. The YU20 and MD18 showed the best performance



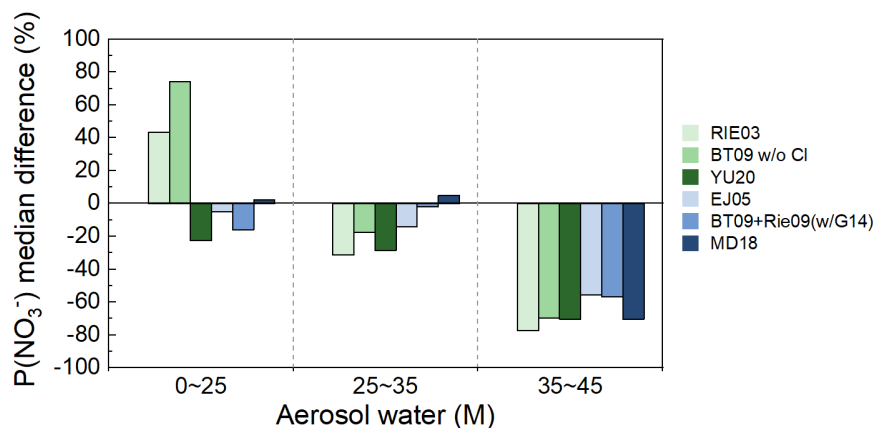
357 across all three ALWC levels among inorganic-only parameterizations and
 358 inorganic+organic parameterizations, respectively. As a result, the overestimation at
 359 low ALWC and underestimation at high ALWC indicated that treatments of ALWC-
 360 related coefficients in most parameterizations can hardly reproduce the response of
 361 $\gamma(\text{N}_2\text{O}_5)$ to ALWC.



362

363 **Figure 5. Comparison of the median values of measured and parameterized**
 364 **$\gamma(\text{N}_2\text{O}_5)$ at low, median and high ALWC levels.** The O/C settings of
 365 BT09+Rie09wG14 and MD18 were 0.8 and 0.5, respectively.

366 The biased prediction of $\gamma(\text{N}_2\text{O}_5)$ at low and high ALWC levels might cause
 367 considerable uncertainties on estimating impacts of N_2O_5 uptake when ALWC varies
 368 largely in ambient conditions. We calculated the particulate nitrate production potential
 369 contributed by N_2O_5 uptake based on measured $\gamma(\text{N}_2\text{O}_5)$ and six selected
 370 parameterizations at low and high ALWC levels, respectively. The maximum deviations
 371 of median nitrate production rates were 74% and -77% at low and high ALWC levels,
 372 respectively (Figure 6). Our results indicate that current parameterizations may lead to
 373 large deviations of nitrate production potential predictions. The contribution of the
 374 N_2O_5 heterogeneous reaction to nitrate production is important in some regions (Wang
 375 et al., 2021; Chen et al., 2020a; Fan et al., 2020; Wagner et al., 2013), and can be
 376 comparable with that of $\text{OH}+\text{NO}_2$ pathway (Alexander et al., 2020; Fan et al., 2022; Zhai
 377 et al., 2023). Therefore, we suggest more $\gamma(\text{N}_2\text{O}_5)$ measurements need to be conducted
 378 under extreme ALWC conditions in future studies, which helps to improve the accuracy
 379 of response coefficients.



380

381 **Figure 6. The median difference of the nitrate production rates $P(\text{NO}_3^-)$ between**
 382 **measured and parameterized $\gamma(\text{N}_2\text{O}_5)$ values during low, median and high ALWC**
 383 **conditions. The O/C setting of BT09+Rie09wG14 was 0.8 and that of MD18 was 0.5.**

384 4. Conclusions

385 The $\gamma(\text{N}_2\text{O}_5)$ on ambient aerosols were directly measured in Kunming by an
 386 aerosol flow tube system. The observed values showed good correlations with organics,
 387 ALWC and aerosol nitrate. The median of $\gamma(\text{N}_2\text{O}_5)$ predicted by inorganic-only and
 388 inorganic+organic parameterizations generally overestimate and underestimate the
 389 measurements, respectively. While some parameterizations agreed well with the
 390 measurements on median values, they failed to reproduce the varying range and showed
 391 low correlations. In particular, parameterizations overestimate the $\gamma(\text{N}_2\text{O}_5)$ by 34~189%
 392 at low ALWC and underestimate by -37%~-1% at high ALWC, respectively. Among
 393 the ten parameterizations, the empirical parameterizations YU20 and MD18 performed
 394 relatively well with lower deviations on median values and RMSE. Our result uncovers
 395 the feasibility of fitting with ambient measurements to improve laboratory-derived
 396 parameterizations. Therefore, we call for the need to conduct more field observations
 397 of $\gamma(\text{N}_2\text{O}_5)$ directly on ambient aerosols to improve the performance of
 398 parameterizations and better elucidate the environmental impacts of N_2O_5 uptake
 399 reaction. Meanwhile, further studies on mechanism of N_2O_5 uptake under extreme
 400 ALWC conditions would help to improve the accuracy of its response coefficients in
 401 parameterizations.

402



403 **Author information**

404 **Corresponding Authors**

405 **Keding Lu** – State Key Joint Laboratory of Environmental Simulation and Pollution
406 Control, College of Environmental Science and Engineering, Peking University,
407 Beijing 100871, China; Email: k.lu@pku.edu.cn

408 **Xiaorui Chen** – School of Atmospheric Sciences, Sun Yat-sen University, and
409 Southern Marine Science and Engineering Guangdong Laboratory (Zhuhai),
410 Zhuhai, 519082, China; Email: chenxr95@mail.sysu.edu.cn

411 **Authors**

412 **Jiayin Li**⁺ – State Key Joint Laboratory of Environmental Simulation and Pollution
413 Control, College of Environmental Science and Engineering, Peking University,
414 Beijing 100871, China

415 **Tianyu Zhai**⁺ – State Key Joint Laboratory of Environmental Simulation and
416 Pollution Control, College of Environmental Science and Engineering, Peking
417 University, Beijing 100871, China; State Environmental Protection Key
418 Laboratory of Vehicle Emission Control and Simulation, Chinese Research
419 Academy of Environmental Sciences, Beijing, 100012, China

420 **Haichao Wang** – School of Atmospheric Sciences, Sun Yat-sen University, and
421 Southern Marine Science and Engineering Guangdong Laboratory (Zhuhai),
422 Zhuhai, 519082, China

423 **Shuyang Xie** – State Key Joint Laboratory of Environmental Simulation and
424 Pollution Control, College of Environmental Science and Engineering, Peking
425 University, Beijing 100871, China

426 **Shiyi Chen** – State Key Joint Laboratory of Environmental Simulation and Pollution
427 Control, College of Environmental Science and Engineering, Peking University,
428 Beijing 100871, China

429 **Chunmeng Li** – State Key Joint Laboratory of Environmental Simulation and
430 Pollution Control, College of Environmental Science and Engineering, Peking



431 University, Beijing 100871, China; The National Institute of Metrology, Center for
432 Environmental Metrology, Beijing 100029, China

433 **Huabin Dong**– State Key Joint Laboratory of Environmental Simulation and
434 Pollution Control, College of Environmental Science and Engineering, Peking
435 University, Beijing 100871, China

436 **Author Contributions**

437 X.R.C. and K.D.L. designed the study. K.D.L. organized the field campaign with the
438 help from Y.J.G. T.Y.Z and X.R.C measured the $\gamma(\text{N}_2\text{O}_5)$ data. C.M.L, S.Y.X, H.B.D
439 and S.Y.C provide the field data of normal gases, particulate components and other
440 supporting parameters. J.Y.L, T.Y.Z, X.R.C and H.C.W analyze the data. J.Y.L, T.Y.Z
441 and X.R.C wrote the paper with the input from K.D.L.

442 **Competing Interests**

443 The authors declare no competing financial interest.

444

445 **Acknowledgments**

446 This work was supported by the National Natural Science Foundation of China
447 (Grants No. 22221004 and No. 22406204).

448

449 **References**

450 Abbatt, J. P. D., Lee, A. K. Y., and Thornton, J. A.: Quantifying trace gas uptake
451 to tropospheric aerosol: recent advances and remaining challenges, *Chemical Society*
452 *Reviews*, 41, 6555-6581, 10.1039/c2cs35052a, 2012.

453 Alexander, B., Sherwen, T., Holmes, C. D., Fisher, J. A., Chen, Q., Evans, M. J.,
454 and Kasibhatla, P.: Global inorganic nitrate production mechanisms: comparison of a
455 global model with nitrate isotope observations, *Atmospheric Chemistry and Physics*,
456 20, 3859-3877, 10.5194/acp-20-3859-2020, 2020.

457 Anttila, T., Kiendler-Scharr, A., Tillmann, R., and Mentel, T. F.: On the reactive
458 uptake of gaseous compounds by organic-coated aqueous aerosols: Theoretical analysis
459 and application to the heterogeneous hydrolysis of N_2O_5 , *J. Phys. Chem. A*, 110, 10435-
460 10443, 10.1021/jp062403c, 2006.

461 Asaf, D., Pedersen, D., Matveev, V., Peleg, M., Kern, C., Zingler, J., Platt, U., and
462 Luria, M.: Long-Term Measurements of NO_3 Radical at a Semiarid Urban Site: 1.



- 463 Extreme Concentration Events and Their Oxidation Capacity, *Environmental Science*
464 & *Technology*, 43, 9117-9123, 10.1021/es900798b, 2009.
- 465 Atkinson, R., Baulch, D. L., Cox, R. A., Crowley, J. N., Hampson, R. F., Hynes,
466 R. G., Jenkin, M. E., Rossi, M. J., and Troe, J.: Evaluated kinetic and photochemical
467 data for atmospheric chemistry: Volume I - gas phase reactions of O-x, HOx, NOx and
468 SOx species, *Atmospheric Chemistry and Physics*, 4, 1461-1738, 10.5194/acp-4-1461-
469 2004, 2004.
- 470 Bertram, T. H., and Thornton, J. A.: Toward a general parameterization of N₂O₅
471 reactivity on aqueous particles: the competing effects of particle liquid water, nitrate
472 and chloride, *Atmos. Chem. Phys.*, 9, 8351-8363, 10.5194/acp-9-8351-2009, 2009.
- 473 Bertram, T. H., Thornton, J. A., and Riedel, T. P.: An experimental technique for
474 the direct measurement of N₂O₅ reactivity on ambient particles, *Atmospheric*
475 *Measurement Techniques*, 2, 231-242, 10.5194/amt-2-231-2009, 2009a.
- 476 Bertram, T. H., Thornton, J. A., Riedel, T. P., Middlebrook, A. M., Bahreini, R.,
477 Bates, T. S., Quinn, P. K., and Coffman, D. J.: Direct observations of N₂O₅ reactivity
478 on ambient aerosol particles, *Geophysical Research Letters*, 36, 10.1029/2009gl040248,
479 2009b.
- 480 Brown, S. S., Ryerson, T. B., Wollny, A. G., Brock, C. A., Peltier, R., Sullivan, A.
481 P., Weber, R. J., Dube, W. P., Trainer, M., Meagher, J. F., Fehsenfeld, F. C., and
482 Ravishankara, A. R.: Variability in nocturnal nitrogen oxide processing and its role in
483 regional air quality, *Science*, 311, 67-70, 10.1126/science.1120120, 2006.
- 484 Brown, S. S., Dube, W. P., Fuchs, H., Ryerson, T. B., Wollny, A. G., Brock, C. A.,
485 Bahreini, R., Middlebrook, A. M., Neuman, J. A., Atlas, E., Roberts, J. M., Osthoff, H.
486 D., Trainer, M., Fehsenfeld, F. C., and Ravishankara, A. R.: Reactive uptake coefficients
487 for N₂O₅ determined from aircraft measurements during the Second Texas Air Quality
488 Study: Comparison to current model parameterizations, *Journal of Geophysical*
489 *Research-Atmospheres*, 114, 10.1029/2008jd011679, 2009.
- 490 Brown, S. S., and Stutz, J.: Nighttime radical observations and chemistry,
491 *Chemical Society Reviews*, 41, 6405-6447, 10.1039/c2cs35181a, 2012.
- 492 Brown, S. S., Dube, W. P., Tham, Y. J., Zha, Q. Z., Xue, L. K., Poon, S., Wang, Z.,
493 Blake, D. R., Tsui, W., Parrish, D. D., and Wang, T.: Nighttime chemistry at a high
494 altitude site above Hong Kong, *Journal of Geophysical Research-Atmospheres*, 121,
495 2457-2475, 10.1002/2015jd024566, 2016.
- 496 Chang, W. L., Bhave, P. V., Brown, S. S., Riemer, N., Stutz, J., and Dabdub, D.:
497 Heterogeneous Atmospheric Chemistry, Ambient Measurements, and Model
498 Calculations of N₂O₅: A Review, *Aerosol Sci. Technol.*, 45, 665-695,
499 10.1080/02786826.2010.551672, 2011.
- 500 Chang, W. L., Brown, S. S., Stutz, J., Middlebrook, A. M., Bahreini, R., Wagner,
501 N. L., Dube, W. P., Pollack, I. B., Ryerson, T. B., and Riemer, N.: Evaluating N₂O₅
502 heterogeneous hydrolysis parameterizations for CalNex 2010, *Journal of Geophysical*
503 *Research-Atmospheres*, 121, 5051-5070, 10.1002/2015jd024737, 2016.
- 504 Chen, S., Wang, H., Lu, K., Zeng, L., Hu, M., and Zhang, Y.: The trend of surface



- 505 ozone in Beijing from 2013 to 2019: Indications of the persisting strong atmospheric
506 oxidation capacity, *Atmospheric Environment*, 242, 10.1016/j.atmosenv.2020.117801,
507 2020a.
- 508 Chen, X., Wang, H., Zhai, T., Li, C., and Lu, K.: Direct measurement of N_2O_5
509 heterogeneous uptake coefficients on ambient aerosols via an aerosol flow tube system:
510 design, characterization and performance, *Atmospheric Measurement Techniques*, 15,
511 7019-7037, 10.5194/amt-15-7019-2022, 2022.
- 512 Chen, X. R., Wang, H. C., Lu, K. D., Li, C. M., Zhai, T. Y., Tan, Z. F., Ma, X. F.,
513 Yang, X. P., Liu, Y. H., Chen, S. Y., Dong, H. B., Li, X., Wu, Z. J., Hu, M., Zeng, L. M.,
514 and Zhang, Y. H.: Field Determination of Nitrate Formation Pathway in Winter Beijing,
515 *Environmental Science & Technology*, 54, 9243-9253, 10.1021/acs.est.0c00972, 2020b.
- 516 Chen, Y., Wolke, R., Ran, L., Birmili, W., Spindler, G., Schroder, W., Su, H., Cheng,
517 Y. F., Tegen, I., and Wiedensohler, A.: A parameterization of the heterogeneous
518 hydrolysis of N_2O_5 for mass-based aerosol models: improvement of particulate nitrate
519 prediction, *Atmos. Chem. Phys.*, 18, 673-689, 10.5194/acp-18-673-2018, 2018.
- 520 Cosman, L. M., and Bertram, A. K.: Reactive uptake of N_2O_5 on aqueous H_2SO_4
521 solutions coated with 1-component and 2-component monolayers, *J. Phys. Chem. A*,
522 112, 4625-4635, 10.1021/jp8005469, 2008.
- 523 Davis, J. M., Bhave, P. V., and Foley, K. M.: Parameterization of N_2O_5 reaction
524 probabilities on the surface of particles containing ammonium, sulfate, and nitrate,
525 *Atmos. Chem. Phys.*, 8, 5295-5311, 10.5194/acp-8-5295-2008, 2008.
- 526 Decker, Z. C. J., Zarzana, K. J., Coggon, M., Min, K. E., Pollack, I., Ryerson, T.
527 B., Peischl, J., Edwards, P., Dubé, W. P., Markovic, M. Z., Roberts, J. M., Veres, P. R.,
528 Graus, M., Warneke, C., de Gouw, J., Hatch, L. E., Barsanti, K. C., and Brown, S. S.:
529 Nighttime Chemical Transformation in Biomass Burning Plumes: A Box Model
530 Analysis Initialized with Aircraft Observations, *Environmental Science & Technology*,
531 53, 2529-2538, 10.1021/acs.est.8b05359, 2019.
- 532 Dentener, F. J., and Crutzen, P. J.: Reaction of N_2O_5 on Tropospheric Aerosols -
533 Impact on the Global Distributions of NO_x , O_3 , and OH, *Journal of Geophysical*
534 *Research-Atmospheres*, 98, 7149-7163, 10.1029/92jd02979, 1993.
- 535 Escoreia, E. N., Sjostedt, S. J., and Abbatt, J. P. D.: Kinetics of N_2O_5 Hydrolysis
536 on Secondary Organic Aerosol and Mixed Ammonium Bisulfate-Secondary Organic
537 Aerosol Particles, *Journal of Physical Chemistry A*, 114, 13113-13121,
538 10.1021/jp107721v, 2010.
- 539 Evans, M. J., and Jacob, D. J.: Impact of new laboratory studies of N_2O_5 hydrolysis
540 on global model budgets of tropospheric nitrogen oxides, ozone, and OH, *Geophys.*
541 *Res. Lett.*, 32, 10.1029/2005gl022469, 2005.
- 542 Fan, M.-Y., Zhang, Y.-L., Lin, Y.-C., Cao, F., Zhao, Z.-Y., Sun, Y., Qiu, Y., Fu, P.,
543 and Wang, Y.: Changes of Emission Sources to Nitrate Aerosols in Beijing After the
544 Clean Air Actions: Evidence From Dual Isotope Compositions, *Journal of Geophysical*
545 *Research-Atmospheres*, 125, 10.1029/2019jd031998, 2020.
- 546 Fan, M. Y., Zhang, Y. L., Lin, Y. C., Hong, Y. H., Zhao, Z. Y., Xie, F., Du, W., Cao,



- 547 F., Sun, Y. L., and Fu, P. Q.: Important Role of NO_3 Radical to Nitrate Formation Aloft
548 in Urban Beijing: Insights from Triple Oxygen Isotopes Measured at the Tower,
549 *Environmental Science & Technology*, 56, 6870-6879, 10.1021/acs.est.1c02843, 2022.
- 550 Fang, Y.-G., Tang, B., Yuan, C., Wan, Z., Zhao, L., Zhu, S., Francisco, J. S., Zhu,
551 C., and Fang, W.-H.: Mechanistic insight into the competition between interfacial and
552 bulk reactions in microdroplets through N_2O_5 ammonolysis and hydrolysis, *Nature*
553 *Communications*, 15, 2347, 10.1038/s41467-024-46674-1, 2024.
- 554 Finlaysonpitts, B. J., Ezell, M. J., and Pitts, J. N.: Formation of chemically active
555 chlorine compounds by reactions of atmospheric nacl particles with gaseous N_2O_5 and
556 ClONO_2 , *Nature*, 337, 241-244, 10.1038/337241a0, 1989.
- 557 Folkers, M., Mentel, T. F., and Wahner, A.: Influence of an organic coating on the
558 reactivity of aqueous aerosols probed by the heterogeneous hydrolysis of N_2O_5 ,
559 *Geophysical Research Letters*, 30, 10.1029/2003gl017168, 2003.
- 560 Fountoukis, C., and Nenes, A.: ISORROPIA II:: a computationally efficient
561 thermodynamic equilibrium model for K^+ - Ca^{2+} - Mg^{2+} - NH_4^+ - Na^+ - SO_4^{2-} - NO_3^- - Cl^- - H_2O
562 aerosols, *Atmospheric Chemistry and Physics*, 7, 4639-4659, 10.5194/acp-7-4639-
563 2007, 2007.
- 564 Gaston, C. J., Thornton, J. A., and Ng, N. L.: Reactive uptake of N_2O_5 to internally
565 mixed inorganic and organic particles: the role of organic carbon oxidation state and
566 inferred organic phase separations, *Atmos. Chem. Phys.*, 14, 5693-5707, 10.5194/acp-
567 14-5693-2014, 2014.
- 568 Griffiths, P. T., Badger, C. L., Cox, R. A., Folkers, M., Henk, H. H., and Mentel,
569 T. F.: Reactive Uptake of N_2O_5 by Aerosols Containing Dicarboxylic Acids. Effect of
570 Particle Phase, Composition, and Nitrate Content, *J. Phys. Chem. A*, 113, 5082-5090,
571 10.1021/jp8096814, 2009.
- 572 Hallquist, M., Stewart, D. J., Stephenson, S. K., and Cox, R. A.: Hydrolysis of
573 N_2O_5 on sub-micron sulfate aerosols, *Physical Chemistry Chemical Physics*, 5, 3453-
574 3463, 10.1039/b301827j, 2003.
- 575 Li, Z. Y., Xie, P. H., Hu, R. Z., Wang, D., Jin, H. W., Chen, H., Lin, C., and Liu,
576 W. Q.: Observations of N_2O_5 and NO_3 at a suburban environment in Yangtze river delta
577 in China: Estimating heterogeneous N_2O_5 uptake coefficients, *J. Environ. Sci.*, 95, 248-
578 255, 10.1016/j.jes.2020.04.041, 2020.
- 579 Liu, X. G., Gu, J. W., Li, Y. P., Cheng, Y. F., Qu, Y., Han, T. T., Wang, J. L., Tian,
580 H. Z., Chen, J., and Zhang, Y. H.: Increase of aerosol scattering by hygroscopic growth:
581 Observation, modeling, and implications on visibility, *Atmospheric Research*, 132, 91-
582 101, 10.1016/j.atmosres.2013.04.007, 2013.
- 583 McDuffie, E. E., Fibiger, D. L., Dube, W. P., Lopez-Hilfiker, F., Lee, B. H.,
584 Thornton, J. A., Shah, V., Jaegle, L., Guo, H. Y., Weber, R. J., Reeves, J. M., Weinheimer,
585 A. J., Schroder, J. C., Campuzano-Jost, P., Jimenez, J. L., Dibb, J. E., Veres, P., Ebben,
586 C., Sparks, T. L., Wooldridge, P. J., Cohen, R. C., Hornbrook, R. S., Apel, E. C., Campos,
587 T., Hall, S. R., Ullmann, K., and Brown, S. S.: Heterogeneous N_2O_5 Uptake During
588 Winter: Aircraft Measurements During the 2015 WINTER Campaign and Critical



- 589 Evaluation of Current Parameterizations, *Journal of Geophysical Research-*
590 *Atmospheres*, 123, 4345-4372, 10.1002/2018jd028336, 2018.
- 591 Morgan, W. T., Ouyang, B., Allan, J. D., Aruffo, E., Di Carlo, P., Kennedy, O. J.,
592 Lowe, D., Flynn, M. J., Rosenberg, P. D., Williams, P. I., Jones, R., McFiggans, G. B.,
593 and Coe, H.: Influence of aerosol chemical composition on N₂O₅ uptake: airborne
594 regional measurements in northwestern Europe, *Atmos. Chem. Phys.*, 15, 973-990,
595 10.5194/acp-15-973-2015, 2015.
- 596 Mozurkewich, M., and Calvert, J. G.: Reaction probability of N₂O₅ on Aqueous
597 Aerosols, *J. Geophys. Res.- Atmos.*, 93, 15889-15896, 10.1029/JD093iD12p15889,
598 1988.
- 599 Murray, L. T., Fiore, A. M., Shindell, D. T., Naik, V., and Horowitz, L. W.: Large
600 uncertainties in global hydroxyl projections tied to fate of reactive nitrogen and carbon,
601 *Proceedings of the National Academy of Sciences of the United States of America*, 118,
602 ARTN e2115204118
603 10.1073/pnas.2115204118, 2021.
- 604 Ng, N. L., Brown, S. S., Archibald, A. T., Atlas, E., Cohen, R. C., Crowley, J. N.,
605 Day, D. A., Donahue, N. M., Fry, J. L., Fuchs, H., Griffin, R. J., Guzman, M. I.,
606 Herrmann, H., Hodzic, A., Iinuma, Y., Jimenez, J. L., Kiendler-Scharr, A., Lee, B. H.,
607 Luecken, D. J., Mao, J. Q., McLaren, R., Mutzel, A., Osthoff, H. D., Ouyang, B.,
608 Picquet-Varrault, B., Platt, U., Pye, H. O. T., Rudich, Y., Schwantes, R. H., Shiraiwa,
609 M., Stutz, J., Thornton, J. A., Tilgner, A., Williams, B. J., and Zaveri, R. A.: Nitrate
610 radicals and biogenic volatile organic compounds: oxidation, mechanisms, and organic
611 aerosol, *Atmospheric Chemistry and Physics*, 17, 2103-2162, 10.5194/acp-17-2103-
612 2017, 2017.
- 613 Niu, Y. B., Zhu, B., He, L. Y., Wang, Z., Lin, X. Y., Tang, M. X., and Huang, X. F.:
614 Fast Nocturnal Heterogeneous Chemistry in a Coastal Background Atmosphere and Its
615 Implications for Daytime Photochemistry, *Journal of Geophysical Research-*
616 *Atmospheres*, 127, 10.1029/2022jd036716, 2022.
- 617 Osthoff, H. D., Roberts, J. M., Ravishankara, A. R., Williams, E. J., Lerner, B. M.,
618 Sommariva, R., Bates, T. S., Coffman, D., Quinn, P. K., Dibb, J. E., Stark, H.,
619 Burkholder, J. B., Talukdar, R. K., Meagher, J., Fehsenfeld, F. C., and Brown, S. S.:
620 High levels of nitryl chloride in the polluted subtropical marine boundary layer, *Nature*
621 *Geoscience*, 1, 324-328, 10.1038/ngeo177, 2008.
- 622 Phillips, G. J., Thieser, J., Tang, M. J., Sobanski, N., Schuster, G., Fachinger, J.,
623 Drewnick, F., Borrmann, S., Bingemer, H., Lelieveld, J., and Crowley, J. N.: Estimating
624 N₂O₅ uptake coefficients using ambient measurements of NO₃, N₂O₅, ClNO₂ and
625 particle-phase nitrate, *Atmos. Chem. Phys.*, 16, 13231-13249, 2016.
- 626 Riedel, T. P., Bertram, T. H., Ryder, O. S., Liu, S., Day, D. A., Russell, L. M.,
627 Gaston, C. J., Prather, K. A., and Thornton, J. A.: Direct N₂O₅ reactivity measurements
628 at a polluted coastal site, *Atmos. Chem. Phys.*, 12, 2959-2968, 10.5194/acp-12-2959-
629 2012, 2012.
- 630 Riedel, T. P., Wolfe, G. M., Danas, K. T., Gilman, J. B., Kuster, W. C., Bon, D. M.,



631 Vlasenko, A., Li, S. M., Williams, E. J., Lerner, B. M., Veres, P. R., Roberts, J. M.,
632 Holloway, J. S., Lefer, B., Brown, S. S., and Thornton, J. A.: An MCM modeling study
633 of nitryl chloride (ClNO₂) impacts on oxidation, ozone production and nitrogen oxide
634 partitioning in polluted continental outflow, *Atmos. Chem. Phys.*, 14, 3789-3800,
635 10.5194/acp-14-3789-2014, 2014.

636 Roberts, J. M., Osthoff, H. D., Brown, S. S., Ravishankara, A. R., Coffman, D.,
637 Quinn, P., and Bates, T.: Laboratory studies of products of N₂O₅ uptake on Cl-
638 containing substrates, *Geophysical Research Letters*, 36, 10.1029/2009gl040448, 2009.

639 Ryder, O. S., Ault, A. P., Cahill, J. F., Guasco, T. L., Riedel, T. P., Cuadra-
640 Rodriguez, L. A., Gaston, C. J., Fitzgerald, E., Lee, C., Prather, K. A., and Bertram, T.
641 H.: On the Role of Particle Inorganic Mixing State in the Reactive Uptake of N₂O₅ to
642 Ambient Aerosol Particles, *Environmental Science & Technology*, 48, 1618-1627,
643 10.1021/es4042622, 2014.

644 Tham, Y. J., Wang, Z., Li, Q. Y., Yun, H., Wang, W. H., Wang, X. F., Xue, L. K.,
645 Lu, K. D., Ma, N., Bohn, B., Li, X., Kecorius, S., Gross, J., Shao, M., Wiedensohler,
646 A., Zhang, Y. H., and Wang, T.: Significant concentrations of nitryl chloride sustained
647 in the morning: investigations of the causes and impacts on ozone production in a
648 polluted region of northern China, *Atmospheric Chemistry and Physics*, 16, 14959-
649 14977, 10.5194/acp-16-14959-2016, 2016.

650 Tham, Y. J., Wang, Z., Li, Q. Y., Wang, W. H., Wang, X. F., Lu, K. D., Ma, N., Yan,
651 C., Kecorius, S., Wiedensohler, A., Zhang, Y. H., and Wang, T.: Heterogeneous N₂O₅
652 uptake coefficient and production yield of ClNO₂ in polluted northern China: roles of
653 aerosol water content and chemical composition, *Atmos. Chem. Phys.*, 18, 13155-
654 13171, 10.5194/acp-18-13155-2018, 2018.

655 Thornton, J. A., Braban, C. F., and Abbatt, J. P. D.: N₂O₅ hydrolysis on sub-micron
656 organic aerosols: the effect of relative humidity, particle phase, and particle size,
657 *Physical Chemistry Chemical Physics*, 5, 4593-4603, 10.1039/b307498f, 2003.

658 Wagner, N. L., Riedel, T. P., Young, C. J., Bahreini, R., Brock, C. A., Dube, W. P.,
659 Kim, S., Middlebrook, A. M., Ozturk, F., Roberts, J. M., Russo, R., Sive, B., Swarthout,
660 R., Thornton, J. A., VandenBoer, T. C., Zhou, Y., and Brown, S. S.: N₂O₅ uptake
661 coefficients and nocturnal NO₂ removal rates determined from ambient wintertime
662 measurements, *Journal of Geophysical Research-Atmospheres*, 118, 9331-9350,
663 10.1002/jgrd.50653, 2013.

664 Wang, H. C., Chen, J., and Lu, K. D.: Development of a portable cavity-enhanced
665 absorption spectrometer for the measurement of ambient NO₃ and N₂O₅: experimental
666 setup, lab characterizations, and field applications in a polluted urban environment,
667 *Atmospheric Measurement Techniques*, 10, 1465-1479, 10.5194/amt-10-1465-2017,
668 2017a.

669 Wang, H. C., Lu, K. D., Chen, X. R., Zhu, Q. D., Chen, Q., Guo, S., Jiang, M. Q.,
670 Li, X., Shang, D. J., Tan, Z. F., Wu, Y. S., Wu, Z. J., Zou, Q., Zheng, Y., Zeng, L. M.,
671 Zhu, T., Hu, M., and Zhang, Y. H.: High N₂O₅ Concentrations Observed in Urban
672 Beijing: Implications of a Large Nitrate Formation Pathway, *Environmental Science &*



- 673 Technology Letters, 4, 416-420, 10.1021/acs.estlett.7b00341, 2017b.
- 674 Wang, H. C., Lu, K. D., Guo, S., Wu, Z. J., Shang, D. J., Tan, Z. F., Wang, Y. J.,
675 Le Breton, M., Lou, S. R., Tang, M. J., Wu, Y. S., Zhu, W. F., Zheng, J., Zeng, L. M.,
676 Hallquist, M., Hu, M., and Zhang, Y. H.: Efficient N_2O_5 uptake and NO_3 oxidation in
677 the outflow of urban Beijing, *Atmos. Chem. Phys.*, 18, 9705-9721, 10.5194/acp-18-
678 9705-2018, 2018.
- 679 Wang, H. C., Chen, X. R., Lu, K. D., Hu, R. Z., Li, Z. Y., Wang, H. L., Ma, X. F.,
680 Yang, X. P., Chen, S. Y., Dong, H. B., Liu, Y., Fang, X., Zeng, L. M., Hu, M., and Zhang,
681 Y. H.: NO_3 and N_2O_5 chemistry at a suburban site during the EXPLORE-YRD
682 campaign in 2018, *Atmospheric Environment*, 224, 10.1016/j.atmosenv.2019.117180,
683 2020a.
- 684 Wang, H. C., Chen, X. R., Lu, K. D., Tan, Z. F., Ma, X. F., Wu, Z. J., Li, X., Liu,
685 Y. H., Shang, D. J., Wu, Y. S., Zeng, L. M., Hu, M., Schmitt, S., Kiendler-Scharr, A.,
686 Wahner, A., and Zhang, Y. H.: Wintertime N_2O_5 uptake coefficients over the North
687 China Plain, *Science Bulletin*, 65, 765-774, 10.1016/j.scib.2020.02.006, 2020b.
- 688 Wang, H. C., Lu, K. D., Chen, S. Y., Li, X., Zeng, L. M., Hu, M., and Zhang, Y.
689 H.: Characterizing nitrate radical budget trends in Beijing during 2013-2019, *Science*
690 *of the Total Environment*, 795, 10.1016/j.scitotenv.2021.148869, 2021.
- 691 Wang, H. C., Yuan, B., Zheng, E., Zhang, X. X., Wang, J., Lu, K. D., Ye, C. S.,
692 Yang, L., Huang, S., Hu, W. W., Yang, S. X., Peng, Y. W., Qi, J. P., Wang, S. H., He, X.
693 J., Chen, Y. B., Li, T. G., Wang, W. J., Huangfu, Y. B., Li, X. B., Cai, M. F., Wang, X.
694 M., and Shao, M.: Formation and impacts of nitryl chloride in Pearl River Delta,
695 *Atmospheric Chemistry and Physics*, 22, 14837-14858, 10.5194/acp-22-14837-2022,
696 2022.
- 697 Wang, H. C., Wang, H. L., Lu, X., Lu, K. D., Zhang, L., Tham, Y. J., Shi, Z. B.,
698 Aikin, K., Fan, S. J., Brown, S. S., and Zhang, Y. H.: Increased night-time oxidation
699 over China despite widespread decrease across the globe, *Nature Geoscience*,
700 10.1038/s41561-022-01122-x, 2023.
- 701 Wang, X. F., Wang, H., Xue, L. K., Wang, T., Wang, L. W., Gu, R. R., Wang, W.
702 H., Tham, Y. J., Wang, Z., Yang, L. X., Chen, J. M., and Wang, W. X.: Observations of
703 N_2O_5 and ClNO_2 at a polluted urban surface site in North China: High N_2O_5 uptake
704 coefficients and low ClNO_2 product yields, *Atmos. Environ.*, 156, 125-134,
705 10.1016/j.atmosenv.2017.02.035, 2017c.
- 706 Wang, Z., Wang, W. H., Tham, Y. J., Li, Q. Y., Wang, H., Wen, L., Wang, X. F.,
707 and Wang, T.: Fast heterogeneous N_2O_5 uptake and ClNO_2 production in power plant
708 and industrial plumes observed in the nocturnal residual layer over the North China
709 Plain, *Atmos. Chem. Phys.*, 17, 12361-12378, 10.5194/acp-17-12361-2017, 2017d.
- 710 Yan, C., Tham, Y. J., Zha, Q., Wang, X., Xue, L., Dai, J., Wang, Z., and Wang, T.:
711 Fast heterogeneous loss of N_2O_5 leads to significant nighttime NO_x removal and nitrate
712 aerosol formation at a coastal background environment of southern China, *Science of*
713 *the Total Environment*, 677, 637-647, 10.1016/j.scitotenv.2019.04.389, 2019.
- 714 Yan, C., Tham, Y. J., Nie, W., Xia, M., Wang, H. C., Guo, Y. S., Ma, W., Zhan, J.



715 L., Hua, C. J., Li, Y. Y., Deng, C. J., Li, Y. R., Zheng, F. X., Chen, X., Li, Q. Y., Zhang,
716 G., Mahajan, A. S., Cuevas, C. A., Huang, D. D., Wang, Z., Sun, Y. L., Saiz-Lopez, A.,
717 Bianchi, F., Kerminen, V. M., Worsnop, D. R., Donahue, N. M., Jiang, J. K., Liu, Y. C.,
718 Ding, A. J., and Kulmala, M.: Increasing contribution of nighttime nitrogen chemistry
719 to wintertime haze formation in Beijing observed during COVID-19 lockdowns, *Nature*
720 *Geoscience*, 16, 975-+, 10.1038/s41561-023-01285-1, 2023.

721 Yu, C., Wang, Z., Xia, M., Fu, X., Wang, W. H., Tham, Y. J., Chen, T. S., Zheng,
722 P. G., Li, H. Y., Shan, Y., Wang, X. F., Xue, L. K., Zhou, Y., Yue, D. L., Ou, Y. B., Gao,
723 J., Lu, K. D., Brown, S. S., Zhang, Y. H., and Wang, T.: Heterogeneous N_2O_5 reactions
724 on atmospheric aerosols at four Chinese sites: improving model representation of
725 uptake parameters, *Atmos. Chem. Phys.*, 20, 4367-4378, 10.5194/acp-20-4367-2020,
726 2020.

727 Zhai, T. Y., Lu, K. D., Wang, H. C., Lou, S. R., Chen, X. R., Hu, R. Z., and Zhang,
728 Y. H.: Elucidate the formation mechanism of particulate nitrate based on direct radical
729 observations in the Yangtze River Delta summer 2019, *Atmospheric Chemistry and*
730 *Physics*, 23, 2379-2391, 10.5194/acp-23-2379-2023, 2023.

731

732